

Author's accepted manuscript (postprint)

Past and future decline of tropical pelagic biodiversity

Yasuhara, M., Wei, C.-L., Kucera, M., Costello, M. J., Tittensor, D. P., Kiessling, W., Bonebrake, T. C., Tabor, C. R., Feng, R., Baselga, A., Kretschmer, K., Kusumoto, B. & Kubota, Y.

Published in: PNAS
DOI: 10.1073/pnas.1916923117

Available online: 26 May 2020

Citation:

Yasuhara, M., Wei, C.-L., Kucera, M., Costello, M. J., Tittensor, D. P., Kiessling, W., Bonebrake, T. C., Tabor, C. R., Feng, R., Baselga, A., Kretschmer, K., Kusumoto, B. & Kubota, Y. (2020). Past and future decline of tropical pelagic biodiversity. PNAS, 117(23), 12891-12896. doi: 10.1073/pnas.1916923117

This is an Accepted Manuscript of an article published by the National Academy of Sciences in PNAS on 26/05/2020, available online: <https://www.pnas.org/content/pnas/117/23/12891.full.pdf>

Past and future decline of tropical pelagic biodiversity

Moriaki Yasuhara^{1,*†}, Chih-Lin Wei^{2,†}, Michal Kucera³, Mark J. Costello^{4,5}, Derek P. Tittensor^{6,7}, Wolfgang Kiessling⁸, Timothy C. Bonebrake¹, Clay Tabor⁹, Ran Feng⁹, Andrés Baselga¹⁰, Kerstin Kretschmer³, Buntarou Kusumoto¹¹, Yasuhiro Kubota¹¹

¹School of Biological Sciences and Swire Institute of Marine Science, The University of Hong Kong, Kadoorie Biological Sciences Building, Pokfulam Road, Hong Kong SAR, China

²Institute of Oceanography, National Taiwan University, No.1, Section 4, Roosevelt Road, Taipei 106, Taiwan

³MARUM – Center for Marine Environmental Sciences and Faculty of Geosciences, University of Bremen, Bremen, Germany

⁴School of Environment, The University of Auckland, 1142 Auckland, New Zealand

⁵Faculty of Biosciences and Aquaculture, Nord University, Post box 1490, 8049 Bodø, Norway

⁶Department of Biology, Dalhousie University, 1355 Oxford Street, Halifax, Nova Scotia, B3H 4R2 Canada

⁷UN Environment Programme World Conservation Monitoring Centre, Cambridge, CB3 0DL UK

⁸GeoZentrum Nordbayern, Department of Geography and Geosciences, Friedrich-Alexander Universität Erlangen–Nürnberg, Loewenichstraße 28, 91054 Erlangen, Germany

⁹Center for Integrative Geosciences, University of Connecticut, 354 Mansfield Road, Storrs, Connecticut 06269, USA

¹⁰Departamento de Zoología, Genética y Antropología Física, Facultad de Biología, Universidad de Santiago de Compostela, 15782 Santiago de Compostela, Spain

¹¹Faculty of Science, University of the Ryukyus, 1 Senbaru Nishihara, Okinawa 903-0213. Japan

*Correspondence to: moriakiyasuhara@gmail.com or yasuhara@hku.hk

†These authors contributed equally to this study

41 **Abstract:** A major research question concerning global pelagic biodiversity remains
42 unanswered: when did the apparent tropical biodiversity depression [i.e., bimodality of
43 latitudinal diversity gradient (LDG)] begin? The bimodal LDG may be a consequence of recent
44 ocean warming, or of deep-time evolutionary speciation and extinction processes. Using rich
45 time-slice datasets of planktonic foraminifers, we show here that a unimodal (or only weakly-
46 bimodal) diversity gradient, with a plateau in the tropics, occurred during the last ice age and has
47 since then developed into a bimodal gradient through species distribution shifts driven by
48 postglacial ocean warming. The bimodal LDG likely emerged before the Anthropocene (here
49 defined as ~1950) and perhaps ~15,000 years ago, indicating a strong environmental control of
50 tropical diversity even before the start of anthropogenic warming. However, our model
51 projections suggest future anthropogenic warming further diminishes tropical pelagic diversity to
52 a level not seen in millions of years.

53
54 **Significance Statement:** We discovered that the tropical oceanic diversity depression is not a
55 recent phenomenon nor very deep-time in origin, by using a comprehensive global dataset of the
56 calcified shells of planktonic foraminifers, abundant unicellular organisms in the world's oceans
57 which are exceptionally well-preserved in marine sediments as fossils. The diversity decline in
58 the lowest latitudes may have started due to rapid post-ice-age warming around 15,000 years
59 ago. Warming may by the end of this century diminish tropical oceanic diversity to an
60 unprecedented level in human history.

61
62 **One Sentence Summary:** The bimodal pelagic latitudinal diversity gradient, at least in
63 planktonic foraminifers, appears to have emerged from the glacial unimodal gradient through
64 species distribution shifts probably driven by postglacial ocean warming.

65 66 **Introduction**

67 Latitudinal diversity gradients (LDGs), the equatorially-centred parabolic diversity patterns, have
68 been described for over 200 years in terrestrial systems (1-4) and are also well-established in
69 marine environments (5-7). However, there is an increasing recognition that marine LDGs,
70 particularly those in open-ocean systems, tend to have an tropical diversity depression and thus
71 to be bimodal (8-14).

72
73 This current tropical depression is consistent with present-day temperatures being beyond the
74 upper physiological thermal tolerances of some species. An inability of species to tolerate high
75 temperatures or sustained physiological stresses may cause shifts of their latitudinal ranges
76 further poleward as the climate warms. Indeed, a near-future tropical biodiversity decline has
77 been predicted with ongoing human-induced climate warming (15-19), and ecosystem-scale
78 impacts of ocean warming are already evident (20-24).

79
80 Alternatively, or additionally, the current tropical dip in diversity could be explained through an
81 evolutionary mechanism of higher speciation rates and/or lower extinction rates at the edges of
82 the tropics (8, 13). Distinguishing the ecological and evolutionary time-scale processes

83 responsible for observed variations in the shape of marine LDGs is critical for assessing the
84 outcome of biotic responses to rapid anthropogenic warming over the coming century (12).
85 However, the lack of a standardized paleoecological baseline for the pelagic LDG has
86 compromised separating whether the observed bimodality is caused by a rapid ecological
87 response to ocean warming, by a longer-term and slower evolutionary process, or both (e.g., 14).
88 While several paleontological studies have shown deep-time bimodal LDGs (25), they are not
89 directly comparable to the present-day pelagic bimodality, or do not answer this question directly
90 for various reasons, including that they tend to be from other (e.g., terrestrial) systems or too
91 deep time to evaluate the hypothesis of rapid ecological response, and/or affected by limited data
92 coverage.

93
94 The calcified shells of planktonic foraminifers, abundant and widespread protists in the world's
95 oceans, are well-preserved in marine sediments and can thus provide a baseline for tracking
96 trends in the LDG over the geologic past (26, 27). In addition, the relationship to temperature of
97 planktonic foraminiferal diversity is consistent with that of many other open ocean organisms (5,
98 11, 28). Here we use global datasets of pre-industrial (broadly representing a late Holocene
99 situation; see Materials and Methods) and last-ice-age planktonic foraminifers as well as a future
100 diversity projection to provide empirical evidence that the tropical diversity depression is neither
101 a recent anthropogenic phenomenon nor of deep-time origin. Rather, it was likely caused by a
102 post-ice-age warming, suggesting a major role for distributional shifts driven by climate.

104 **Results and Discussion**

105 *Diversity patterns with latitude and temperature*

106 Our global analysis of planktonic foraminiferal diversity [calculated as species richness (Hill
107 number, $q = 0$) and effective number of common species (Hill number, $q = 1$), see Materials and
108 Methods] demonstrates that during the Last Glacial Maximum (LGM, ca. 21 kyr ago), the LDG
109 was unimodal (or only weakly bimodal), whereas the pre-industrial LDG was bimodal with a
110 distinct tropical diversity depression (Fig. 1, SI Appendix, Fig. S1, Tables S1, S2). This indicates
111 that the strength of the bimodal LDG for planktonic foraminifers cannot be entirely due to long-
112 term evolutionary processes because it was minimal during the LGM (Fig. 1, SI Appendix, Fig.
113 S1, Tables S1, S2), and there have been no known global extinctions or speciations of any
114 planktonic foraminiferal species since the LGM (29).

115
116 We propose that the cause of the bimodality may then be environmentally-driven extirpation
117 and/or immigration. During warming, any diversity losses at higher latitudes (due to range shifts
118 of species to even higher latitudes) are compensated for by the poleward movements of species
119 from lower latitudes. However, in the tropics, such compensation due to species range shifts is
120 not possible, resulting in an tropical diversity decline (15, 17, 30, 31).

121
122 It is unlikely that the tropical diversity depression is a very recent phenomenon originating in the
123 Anthropocene, because we found that the pre-industrial LDG was already bimodal. Thus, the
124 bimodal LDG most likely developed during the post-LGM warming, with a 5.2 % loss in the

125 mean projected species richness since the LGM at the equator (calculated based on the mean
126 predictions within ± 1 degree latitude; Fig. 1).

127
128 The LDG exhibited a tropical plateau (or weak bimodality) during the LGM (Fig. 1, SI
129 Appendix, Fig. S1) indicating an approach towards diversity saturation (at or beyond the
130 optimum in the unimodal temperature-diversity relationship; see the next paragraph) with
131 relatively low maximum global sea temperature. The distinct tropical diversity decline may have
132 begun $\sim 15,000$ years ago, given that a rapid postglacial warming started at that time (32). The
133 duration of glacial periods has been much longer than that of interglacial periods during the late
134 Quaternary. Therefore, the tropical thermal niches of marine organisms may be optimized to the
135 maximum temperatures of glacial periods, leading to tropical diversity depressions during warm
136 periods, given marine niche conservatism is known to have existed during late Quaternary
137 climate changes (33). As a bimodal LDG is known to be present during the last interglacial (in
138 corals; 34), it is likely that the bimodal LDG has appeared repeatedly during warm interglacial
139 periods during the late Quaternary, and weakened during glacial periods. Species adapted to very
140 warm temperatures existed during the Pliocene, the major previous warmer-than-present period,
141 but significant extinctions of these species are known during the Plio-Pleistocene cooling (27).
142 Note that pre-Plio-Pleistocene Phanerozoic LDG are also known to be dynamic (14, 35-37)
143 though the underlying mechanism may be different.

144
145 Sea surface temperature has been and is unimodal with latitude (Fig. 2d, but see the next
146 paragraph for the equatorial upwelling zone). It is also predicted to remain unimodal under the
147 RCP 8.5 'business-as-usual' climate warming scenario in 2091-2100 ('2090s' hereafter), with
148 $\sim 0-4$ degrees warming relative to the pre-industrial control (PIC) (Fig. 2). The magnitude of the
149 predicted warming from the PIC to the RCP 8.5 2090s will be larger (and much more rapid) than
150 that from the LGM to PIC (Fig. 2), particularly in the tropics. The unimodal (or only weakly
151 bimodal) LDG during the LGM and the bimodal LDG during the pre-industrial time period
152 reflect a positive temperature-diversity relationship from -2°C to 20°C and a negative
153 relationship beyond that, especially beyond 25°C and for species richness (SI Appendix, Fig.
154 S2). Thus, the present reduction of species diversity in the tropics is likely due to high sea
155 temperatures (SI Appendix, Fig. S2), a thermal response also identified in other pelagic groups
156 (38). Such very high temperatures (those exceeding 25°C) did not exist in any latitudinal band
157 during the LGM (Fig. 2). Supporting our interpretation is the observation that planktonic
158 foraminifer species tend to have optimum temperature ranges at $\sim 20-30^{\circ}\text{C}$, with a sharp drop in
159 their growth rates above these temperatures, showing a high-end temperature threshold of
160 thermal performance curves (19, 39, 40). Using the relationship between sea surface temperature
161 and diversity for both time periods (LGM and PIC), we predict a more than 15 % diversity loss
162 at the equator (calculated based on the mean predictions within ± 1 degree latitude) within this
163 century under the 'business-as-usual' climate warming scenario (Fig. 1, SI Appendix, Fig. S1).
164 In comparison, only ~ 5 % diversity loss at the equator has been observed between the LGM and
165 PIC (Fig. 1, SI Appendix, Fig. S1), indicating the potential for a three times greater reduction
166 over the coming century. It is also noteworthy that corals had a bimodal LDG in the last
167 interglacial, a warmer-than-present time period (34). Thus, we may see tropical diversity decline
168 not only in planktonic foraminifers but also in other taxonomic and functional groups with
169 further future warming.

170

171 In the equatorial upwelling zone of the eastern Pacific Ocean (especially at ~100–120 °W; Fig.
172 2b), sea surface temperature is lower than that in adjacent higher-latitude (e.g., 5–10 °N and °S)
173 tropical waters, which may affect species diversity. Indeed, the equatorial diversity is higher than
174 that at 5–10 °N and °S in the eastern Pacific at ~100–120 °W (Fig. 1b). Thus, in the present-day
175 ocean, the equatorial upwelling zone with lower temperature than adjacent higher-latitude
176 tropical waters may be within or close to the optimum temperature range of many species and act
177 as a refugium. In the future warmer ocean, however, temperature will be beyond the optimum
178 temperature range even in the equatorial upwelling zone (Fig. 2c) and the refugium will
179 disappear (Fig. 1c). Nonetheless, the equatorial upwelling zone does not affect our major results,
180 because the low temperature zone related to the equatorial upwelling is limited to a very narrow
181 equatorial band of the eastern Pacific Ocean. The analyses of just the Atlantic Ocean, which
182 lacks a distinct equatorial temperature decline, show the same basic results (see Materials and
183 Methods).

184

185 Higher latitude, especially temperate, diversity increases from the LGM to PIC and from the PIC
186 to RCP 8.5 2090s and offsets the tropical diversity decline (Fig. 3). The temperate peaks of
187 diversity shift poleward in the comparison between the PIC and RCP 8.5 2090s (Fig. 3b) relative
188 to that between the LGM and PIC (Fig. 3a), indicating that future warming will further enhance
189 poleward species range shifts. Both the tropical diversity decline and temperate diversity
190 increase from the PIC to 2090s would be reduced with the low-emission scenario RCP 2.6
191 relative to the business-as-usual scenario RCP 8.5 (Fig. 3c). The subpolar diversity decline from
192 the PIC to 2090s (negative Δ diversity peak at ~50–60 °N; Fig. 3b, c) is probably due to
193 projected subpolar North Atlantic cooling related to a collapse of the local deep-ocean
194 convection (41-43).

195

196 ***Beta-diversity and the process of diversity change***

197 Beta-diversity quantifies how species composition changes in space and time; for example in
198 response to temperature gradients and ocean warming. We divided beta diversity into turnover
199 and nestedness components (Fig. 4, see Materials and Methods). Turnover occurs with species
200 replacement along an environmental gradient, and nestedness indicates species loss without
201 replacement; i.e., when an assemblage is a subset of a more species rich neighbouring biota. The
202 relative contributions of turnover and nestedness components had positive and negative peaks
203 respectively in the tropics during the LGM, showing unimodal and inverse unimodal LDGs (Fig.
204 4). Since then the peaks have moved poleward towards the edges of the tropics, showing bimodal
205 and inverse bimodal LDGs during the pre-industrial time (Fig. 4). The tropical peak of the pre-
206 industrial inverse bimodal nestedness LDG is due to a reduction of species, presumably those
207 most sensitive to the warming. In other words, the pre-industrial tropical assemblage has lost
208 species and has become more of a subset of the adjacent higher-latitude tropical assemblages.
209 The peaks in relative contribution of turnover (positive) and nestedness (negative) to beta
210 diversity at the edges of the pre-industrial tropics (Fig. 4) indicate distributional shifts of some of
211 tropical species, which had an equatorial distribution during the LGM, towards higher latitudes
212 (SI Appendix, Fig. S3). Overall, 23 of 27 species extended their interquartile range (75-25
213 percentile) and shifted southern and northern edges of distributions (97.5-2.5 percentiles)

214 poleward since the LGM, and 6 of 27 species show much stronger bimodal latitudinal
215 distributions of their occurrence density in the PIC than in the LGM, which is probably
216 responsible for the observed bimodal PIC LDG (SI Appendix, Fig. S3).

217

218 *Future scenario*

219 A future tropical diversity depression has not only been predicted for planktonic foraminifers but
220 also for other taxonomic and functional groups (Fig. 1; 8, 9, 11, 18, 19). Planktonic foraminifer
221 diversity is known to track marine and especially pelagic diversity (5, 26). Given the exceptional
222 fossil record of planktonic foraminifers used here as an ideal model system and the fact that most
223 marine organisms have poor fossil records, our findings may further apply to other taxonomic
224 groups. For example, Kaschner et al. (44) suggested a reduction of tropical and an increase in
225 temperate diversity in marine mammals under a warming scenario.

226

227 In a warmer pelagic world, temperate regions will hold more tropical species, and polar regions
228 more temperate species, as they change their distributions to live within their optimum
229 temperature niches (16). However, tropical regions will have no source for such immigrants (16-
230 18). Our study shows that this tropical dead-end causes a local diversity reduction of planktonic
231 foraminifers between 20 °S and °N. The situation will worsen with continued global warming in
232 the coming decades, particularly without appropriate mitigation of greenhouse gas emissions
233 (Fig. 3c). This tropical pelagic diversity decline likely emerged before industrialization and the
234 Anthropocene and perhaps during the onset of the postglacial warming ~15,000 years ago.
235 Future anthropogenic warming may diminish tropical diversity to a level not seen in millions of
236 years.

237

238

239

References

- 240 1. Bonebrake TC (2013) Conservation implications of adaptation to tropical climates from a
241 historical perspective. *J Biogeogr* 40:409-414.
- 242 2. Fine PVA (2015) Ecological and evolutionary drivers of geographic variation in species
243 diversity. *The Annual Review of Ecology, Evolution, and Systematics* 46:369–392.
- 244 3. Hillebrand H (2004) On the generality of the latitudinal diversity gradient. *Am Nat*
245 163:192-211.
- 246 4. Willig MR, Kaufman DM, Stevens RD (2003) Latitudinal gradients of biodiversity:
247 pattern, process, scale, and synthesis. *Annual Review of Ecology, Evolution, and*
248 *Systematics* 34:273–309.
- 249 5. Tittensor DP, *et al.* (2010) Global patterns and predictors of marine biodiversity across
250 taxa. *Nature* 466:1098-1101.
- 251 6. Beaugrand G, Rombouts I, Kirby RR (2013) Towards an understanding of the pattern of
252 biodiversity in the oceans. *Global Ecology and Biogeography* 22:440–449.
- 253 7. Hillebrand H (2004) Strength, slope and variability of marine latitudinal gradients. *Mar*
254 *Ecol Prog Ser* 273:251–267.
- 255 8. Chaudhary C, Saeedi H, Castello MJ (2016) Bimodality of latitudinal gradients in marine
256 species richness. *Trends Ecol Evol* 31:670–676.
- 257 9. Chaudhary C, Saeedi H, Costello MJ (2017) Marine species richness is bimodal with
258 latitude: A reply to Fernandez and Marques. *Trends Ecol Evol* 32:234–237.
- 259 10. Saeedi H, Dennis TE, Costello MJ (2017) Bimodal latitudinal species richness and high
260 endemism of razor clams (Mollusca). *J Biogeogr* 44:592–604.
- 261 11. Rutherford S, D'Hondt S, Prell W (1999) Environmental controls on the geographic
262 distribution of zooplankton diversity. *Nature* 400:749–753.
- 263 12. Worm B, Tittensor DP (2018) *A Theory of Global Biodiversity* (Princeton University
264 Press, Princeton).
- 265 13. Brayard A, Escarguel G, Bucher H (2005) Latitudinal gradient of taxonomic richness:
266 combined outcome of temperature and geographic mid-domains effects? *J Zool Syst Evol*
267 *Res* 43:178–188.
- 268 14. Powell MG, Beresford VP, Colaianne BA (2012) The latitudinal position of peak marine
269 diversity in living and fossil biotas. *J Biogeogr* 39:1687–1694.
- 270 15. Beaugrand G, Edwards M, Raybaud V, Goberville E, Kirby RR (2015) Future
271 vulnerability of marine biodiversity compared with contemporary and past changes. *Nat*
272 *Clim Change* 5:695–701.

- 273 16. Cheung WWL, Pauly D (2016) Impacts and effects of ocean warming on marine fishes.
274 in *Explaining Ocean Warming: Causes, scale, effects and consequences*, eds Laffoley D,
275 Baxter JM (IUCN, Gland), pp 239–253.
- 276 17. Cheung WWL, Watson R, Pauly D (2013) Signature of ocean warming in global fisheries
277 catch. *Nature* 497:365–368.
- 278 18. García Molinos J, *et al.* (2016) Climate velocity and the future global redistribution of
279 marine biodiversity. *Nat Clim Change* 6:83–88.
- 280 19. Roy T, Lombard F, Bopp L, Gehlen M (2015) Projected impacts of climate change and
281 ocean acidification on the global biogeography of planktonic Foraminifera.
282 *Biogeosciences* 12:2873–2889.
- 283 20. Pecl GT, *et al.* (2017) Biodiversity redistribution under climate change: Impacts on
284 ecosystems and human well-being. *Science* 355:doi:10.1126/science.aai9214
- 285 21. Wernberg T, *et al.* (2016) Climate-driven regime shift of a temperate marine ecosystem.
286 *Science* 353:169–172.
- 287 22. Poloczanska ES, *et al.* (2013) Global imprint of climate change on marine life. *Nat Clim*
288 *Change* 3:919–925.
- 289 23. Ainsworth TD, *et al.* (2016) Climate change disables coral bleaching protection on the
290 Great Barrier Reef. *Science* 352:338–342.
- 291 24. Field DB, Baumgartner TR, Charles CD, Ferreira-Bartrina V, Ohman MD (2006)
292 Planktonic foraminifera of the California Current reflect 20th-century warming. *Science*
293 311:63–66.
- 294 25. Mannion PD, Upchurch P, Benson RBJ, Goswami A (2014) The latitudinal biodiversity
295 gradient through deep time. *Trends Ecol Evol* 29:42–50.
- 296 26. Yasuhara M, *et al.* (2017) Cenozoic dynamics of shallow-marine biodiversity in the
297 Western Pacific. *Journal of Biogeography* 44:567–578.
- 298 27. Yasuhara M, Hunt G, Dowsett HJ, Robinson MM, Stoll DK (2012) Latitudinal species
299 diversity gradient of marine zooplankton for the last three million years. *Ecology Letters*
300 15:1174–1179.
- 301 28. Fenton IS, Pearson PN, Jones TD, Purvis A (2016) Environmental predictors of diversity
302 in recent planktonic foraminifera as recorded in marine sediments. *Plos One*
303 11:e0165522, 0165510.0161371/journal.pone.0165522.
- 304 29. Aze T, *et al.* (2011) A phylogeny of Cenozoic macroperforate planktonic foraminifera
305 from fossil data. *Biological Reviews* 86:900–927.

- 306 30. Burrows MT, *et al.* (2014) Geographical limits to species-range shifts are suggested by
307 climate velocity. *Nature* 507:492–495.
- 308 31. Sunday JM, Bates AE, Dulvy NK (2012) Thermal tolerance and the global redistribution
309 of animals. *Nat Clim Change* 2:686–690.
- 310 32. North Greenland Ice Core Project members (2004) High resolution record of northern
311 hemisphere climate extending into the last interglacial period. *Nature* 431:147–151.
- 312 33. Waterson AM, Edgar KM, Schmidt DN, Valdes PJ (2017) Quantifying the stability of
313 planktic foraminiferal physical niches between the Holocene and Last Glacial Maximum.
314 *Paleoceanography* 32:74–89.
- 315 34. Kiessling W, Simpson C, Beck B, Mewis H, Pandolfi JM (2012) Equatorial decline of
316 reef corals during the last Pleistocene interglacial. *Proc Natl Acad Sci U S A* 109:21378–
317 21383.
- 318 35. Boersma A, Premoli Silva I (1991) Distribution of Paleogene planktonic foraminifera –
319 analogies with the Recent? *Palaeogeography, Palaeoclimatology, Palaeoecology* 83:29–
320 48.
- 321 36. Fenton IS, *et al.* (2016) The impact of Cenozoic cooling on assemblage diversity in
322 planktonic foraminifera. *Philosophical Transactions of the Royal Society B*
323 371:doi:10.1098/rstb.2015.0224.
- 324 37. Powell MG (2009) The latitudinal diversity gradient of brachiopods over the past 530
325 million years. *Journal of Geology* 117: 585–594.
- 326 38. Boyce DG, Tittensor DP, Worm B (2008) Effects of temperature on global patterns of
327 tuna and billfish richness. *Mar Ecol Prog Ser* 355:267–276.
- 328 39. Lombard F, Labeyrie L, Michel E, Spero HJ, Lea DW (2009) Modelling the temperature
329 dependent growth rates of planktic foraminifera. *Marine Micropaleontology* 70:1–7.
- 330 40. Žarić S, Donner B, Fischer G, Mulitza S, Wefer G (2005) Sensitivity of planktic
331 foraminifera to sea surface temperature and export production as derived from sediment
332 trap data. *Marine Micropaleontology* 55:75–105.
- 333 41. Sgubin G, Swingedouw D, Drijfhout S, Mary Y, Bennabi A (2017) Abrupt cooling over
334 the North Atlantic in modern climate models. *Nat Commun*
335 8:doi:10.1038/ncomms14375.
- 336 42. Drijfhout S, van Oldenburgh GJ, Cimadoribus A (2012) Is a decline of AMOC causing
337 the warming hole above the North Atlantic in observed and modelled warming patterns?
338 *J Climate* 25:8373–8379.
- 339 43. Kim H, An S (2013) On the subarctic North Atlantic cooling due to global warming.
340 *Theoretical and Applied Climatology* 114:9–19.

- 341 44. Kaschner K, Tittensor DP, Ready J, Gerrodette T, Worm B (2011) Current and Future
342 Patterns of Global Marine Mammal Biodiversity. *Plos One*
343 6:doi:10.1371/journal.pone.0019653.
- 344 45. Siccha M, Kucera M (2017) Data Descriptor: ForCenS, a curated database of planktonic
345 foraminifera census counts in marine surface sediment samples. *Ascientific Data*
346 4:170109, doi:170110.171038/sdata.172017.170109.
- 347 46. Kucera M, Rosell-Mele A, Schneider R, Waelbroeck C, Weinelt M (2005) Multiproxy
348 approach for the reconstruction of the glacial ocean surface (MARGO). *Quaternary Sci*
349 *Rev* 24:813–819.
- 350 47. Kucera M, *et al.* (2005) Reconstruction of sea-surface temperatures from assemblages of
351 planktonic foraminifera: multi-technique approach based on geographically constrained
352 calibration data sets and its application to glacial Atlantic and Pacific Oceans.
353 *Quaternary Sci Rev* 24:951–998.
- 354 48. Jonkers L, Hillebrand H, Kucera M (2019) Global change drives modern plankton
355 communities away from the pre-industrial state. *Nature*:doi:10.1038/s41586-41019-
356 41230-41583.
- 357 49. Menegotto A, Rangel TF (2018) Mapping knowledge gaps in marine diversity reveals a
358 latitudinal gradient of missing species richness. *Nat Commun* 9:4713,
359 doi:4710.1038/s41467-41018-07217-41467.
- 360 50. Block K, Mauritsen T (2013) Forcing and feedback in the MPI-ESM-LR coupled model
361 under abruptly quadrupled CO₂. *Journal of Advances in Modeling Earth Systems* 5:676–
362 691.
- 363 51. Dufresne JL, *et al.* (2013) Climate change projections using the IPSL-CM5 Earth System
364 Model: from CMIP3 to CMIP5. *Clim Dynam* 40:2123–2165.
- 365 52. Schmidt GA, *et al.* (2014) Configuration and assessment of the GISS ModelE2
366 contributions to the CMIP5 archive. *Journal of Advances in Modeling Earth Systems*
367 6:141–184.
- 368 53. Dunne JP, *et al.* (2012) GFDL's ESM2 global coupled climate-carbon earth system
369 models. Part I: physical formulation and baseline simulation characteristics. *J Climate*
370 25:6646–6665.
- 371 54. Giorgetta MA, *et al.* (2013) Climate and carbon cycle changes from 1850 to 2100 in
372 MPI-ESM simulations for the Coupled Model Intercomparison Project phase 5. *Journal*
373 *of Advances in Modeling Earth Systems* 5:572–597.
- 374 55. Hill MO (1973) Diversity and evenness: a unifying notation and its consequences.
375 *Ecology* 54:427–473.

- 376 56. Chao A, *et al.* (2018) An attribute-diversity approach to functional diversity, functional
377 beta diversity, and related (dis)similarity measures. *Ecological Monographs*.
- 378 57. Baselga A (2010) Partitioning the turnover and nestedness components of beta diversity.
379 *Global Ecology and Biogeography* 19:134–143.
- 380 58. Baselga A (2012) The relationship between species replacement, dissimilarity derived
381 from nestedness, and nestedness. *Global Ecology and Biogeography* 21:1223–1232.
- 382 59. R Core Team (2018) *R: A language and environment for statistical computing* (R
383 Foundation for Statistical Computing, Vienna).
- 384 60. Oksanen J, *et al.* (2018) vegan: Community Ecology Package. R package version 2.5-2.
385 <https://CRAN.R-project.org/package=vegan>.
- 386 61. Baselga A, Orme CDL (2012) betapart: an R package for the study of beta diversity.
387 *Methods in Ecology and Evolution* 3:808–812.
- 388 62. Wood SN (2017) *Generalized Additive Models: An Introduction with R (2nd edition)*
389 (CRC Press, Boca Raton).
- 390 63. Hijmans RJ (2017) raster: Geographic Data Analysis and Modeling. R package version
391 2.6-7. <https://CRAN.R-project.org/package=raster>.
- 392 64. Bivand RS, Pebesma E, Gomez-Rubio V (2013) *Applied spatial data analysis with R*
393 (2nd edition) (Springer-Verlag, New York).
- 394 65. Wickham H (2016) *ggplot2: Elegant Graphics for Data Analysis* (Springer-Verlag, New
395 York).
- 396 66. Zuur AF (2009) *Mixed effects models and extensions in ecology with R* (Springer-Verlag,
397 New York).
- 398 67. Hoekstra JM, *et al.* (2010) *The Atlas of Global Conservation: Changes, Challenges, and*
399 *Opportunities to Make a Difference* (University of California Press, Berkeley,
400 <https://databasin.org/datasets/fa0b432f713546f2b98b4934265efb2b>).
- 401
- 402

403 **Acknowledgments:** We thank Michael Siccha for helping with the foraminiferal dataset; and the
404 editors and three anonymous reviewers for constructive comments. This project is supported by
405 bioDISCOVERY, Future Earth.

406 **Funding:** The work described in this paper was partially supported by grants from the Research
407 Grants Council of the Hong Kong Special Administrative Region, China (Project No. HKU
408 17302518, HKU 17303115, HKU 709413P), the Seed Funding Programme for Basic Research
409 of the University of Hong Kong (project codes: 201611159053, 201311159076) (to M.Y.), the
410 Ministry of Science Technology Taiwan (MOST 108-2611-M-002-001) (to C.L.W.), the
411 Program for Advancing Strategic International Networks to Accelerate the Circulation of
412 Talented Researchers, the Japan Society for the Promotion of Science (to Y.K.), the Deutsche
413 Forschungsgemeinschaft (DFG: KI 806/16-1, FOR 2332) (to W.K.), and from the Jarislowsky
414 Foundation (to D.P.T.).

415 **Author contributions:** M.Y. conceived and designed the research; M.Y. fixed the research plan
416 details by discussing with Y.K., B.K., C.L.W., M.J.C., and T.C.B. in a workshop in Okinawa;
417 M.K., M.Y., and K.K., contributed to the database establishment and adjustment; C.T., R.F., and
418 C.L.W. contributed to the climate models; C.L.W. performed most of the data analyses with
419 inputs from M.Y., A.B., C.T., R.F., M.J.C., D.P.T., W.K., T.C.B., B.K., and Y.K.; M.Y. prepared
420 the manuscript with input from all authors.

421 **Competing interests:** Authors declare no competing interests.

422 **Data and materials availability:** All data is available through the main text, the supplementary
423 materials, and references therein.

424

425 **Materials and Methods**

426 Foraminifera

427 We used exceptionally comprehensive global census datasets of planktonic foraminifera, the
428 ForCenS (45) and the MARGO (46, 47) compilations, for "present-day" pre-industrial (see
429 below) and LGM LDG reconstructions, respectively. The databases comprise specimens
430 collected using a constant 150 μm sieve size (see Yasuhara et al., 2012 for discussion on the
431 sieve size). We consider *Globigerinoides ruber* pink and white as separate species. We merged
432 *Globorotalia menardii* and *Globorotalia tumida*. P/D integrate is merged with
433 *Neogloboquadrina incompta*. Otherwise, we used species only and did not use subspecies or
434 categories including multiple species. *Globorotalia crassula* was removed from the datasets,
435 because it already became extinct ~0.9 million years ago (28, 29). We also removed small, rare,
436 and/or taxonomically obscure species (*Tenuitella iota*, *Berggrenia pumilio*, *Dentigloborotalia*
437 *anfracta*, *Globorotalia cavernula*, *Globigerinita minuta*, and *Globorotalia ungulata*) following
438 Siccha and Kucera (45). Eventually, we used these 34 species: *Beella digitata*, *Candeina nitida*,
439 *Globigerina bulloides*, *Globigerina falconensis*, *Globigerinella adamsi*, *Globigerinella calida*,
440 *Globigerinella siphonifera*, *Globigerinita glutinata*, *Globigerinita uvula*, *Globigerinoides*
441 *conglobatus*, *Globigerinoides ruber* pink, *Globigerinoides ruber* white, *Globigerinoides tenellus*,
442 *Globoconella inflata*, *Globoquadrina conglomerata*, *Globorotalia crassaformis*, *Globorotalia*
443 *hirsuta*, *Globorotalia menardii+tumida*, *Globorotalia scitula*, *Globorotalia theyeri*, *Globorotalia*
444 *truncatulinoides*, *Globorotaloides hexagonus*, *Globoturborotalita rubescens*, *Hastigerina*
445 *pelagica*, *Hastigerinella digitata*, *Neogloboquadrina dutertrei*, *Neogloboquadrina incompta*,

446 *Neogloboquadrina pachyderma*, *Orbulina universa*, *Pulleniatina obliquiloculata*,
447 *Sphaeroidinella dehiscens*, *Trilobatus sacculifer*, *Turborotalita humilis*, *Turborotalita*
448 *quinqueloba*. After removing duplicated samples, the pre-industrial ForCenS and LGM MARGO
449 datasets include 4138 and 1442 samples, respectively, with >~300 specimens per sample for
450 most samples (45-47). Given generally slow sedimentation rate in the deep sea, the ForCenS
451 coretop "present day" dataset probably represents mostly the late Holocene (= the last few
452 thousand years) but pre-industrial and pre-Anthropocene (48). Although small proportion of
453 specimens would be from the Anthropocene, they should be negligible, given time averaging of a
454 few thousand years. It is unlikely that the bimodal LDGs are artifacts of sampling biases (49),
455 because tropical regions are well sampled in our datasets (Fig. 1, SI Appendix, Fig. S1), and the
456 less sampled LGM dataset does not show a remarkably bimodal LDG.

457 458 Temperature

459 We used the 3-D, fully coupled Earth system models GISS-E2-R from the Goddard Institute for
460 Space Studies, IPSL-CM5A-LR from the Institut Pierre Simon Laplace, and MPI-ESM-P from
461 the Max Planck Institute to calculate the ensemble average of annual mean sea surface
462 temperature (SST) for the last 100 years during the LGM (50-52). For the last 100 years of the
463 pre-industrial control (PIC) scenario and the years 2091-2100 (2090s) projections (RCP 8.5 a.k.a.
464 business-as-usual scenario and RCP 2.6 with appropriate mitigations of carbon dioxide
465 emission), we use earth system model simulations from the Geophysical Fluid Dynamics
466 Laboratory's GFDL-ESM-2G, the Institut Pierre Simon Laplace's IPSL-CM5A-MR, and the
467 Max Planck Institute's MPI-ESM-MR to calculate the ensemble average of the annual mean SST
468 (51, 53, 54). We re-projected the SST layer of each Earth system model to 0.5 by 0.5-degree
469 grids based on bilinear interpolation and then calculated the multi-model average of each
470 interpolated grid. All Earth system models are part of the Coupled Model Intercomparison
471 Project Phase 5 (CMIP5) and were downloaded from the Earth System Grid Federation (ESGF)
472 Peer-to-Peer (P2P) enterprise system (<https://esgf.llnl.gov/>).

473 474 Statistical modeling

475 For diversity measures, we used Hill numbers (55), ${}^qD = (\sum_{i=1}^S p_i^q)^{1/(1-q)}$, where S is the number of
476 species in a site and p_i is the relative abundance of the i th species. The (larger) value of order q
477 discounts the rare species and thus emphasizes the abundant species. When $q = 0$, all species
478 have equal weight and qD is equivalent to species richness. Where q approaches 1, the derived
479 mathematical expression of Hill numbers (1D) is given as ${}^1D = \exp(-\sum_{i=1}^S p_i \log(p_i))$. Because the
480 equation gives more weight to common species (with higher relative abundance), it can be
481 interpreted as the effective number of equally-abundant and common (typical) species in a
482 community (56). Both measures were very similar in our results, so we present the Hill number
483 of order $q = 0$ in the main text because species richness is the most intuitive and commonly used
484 measure of diversity, and $q = 1$ (the exponential form of the Shannon index) in the SI Appendix.

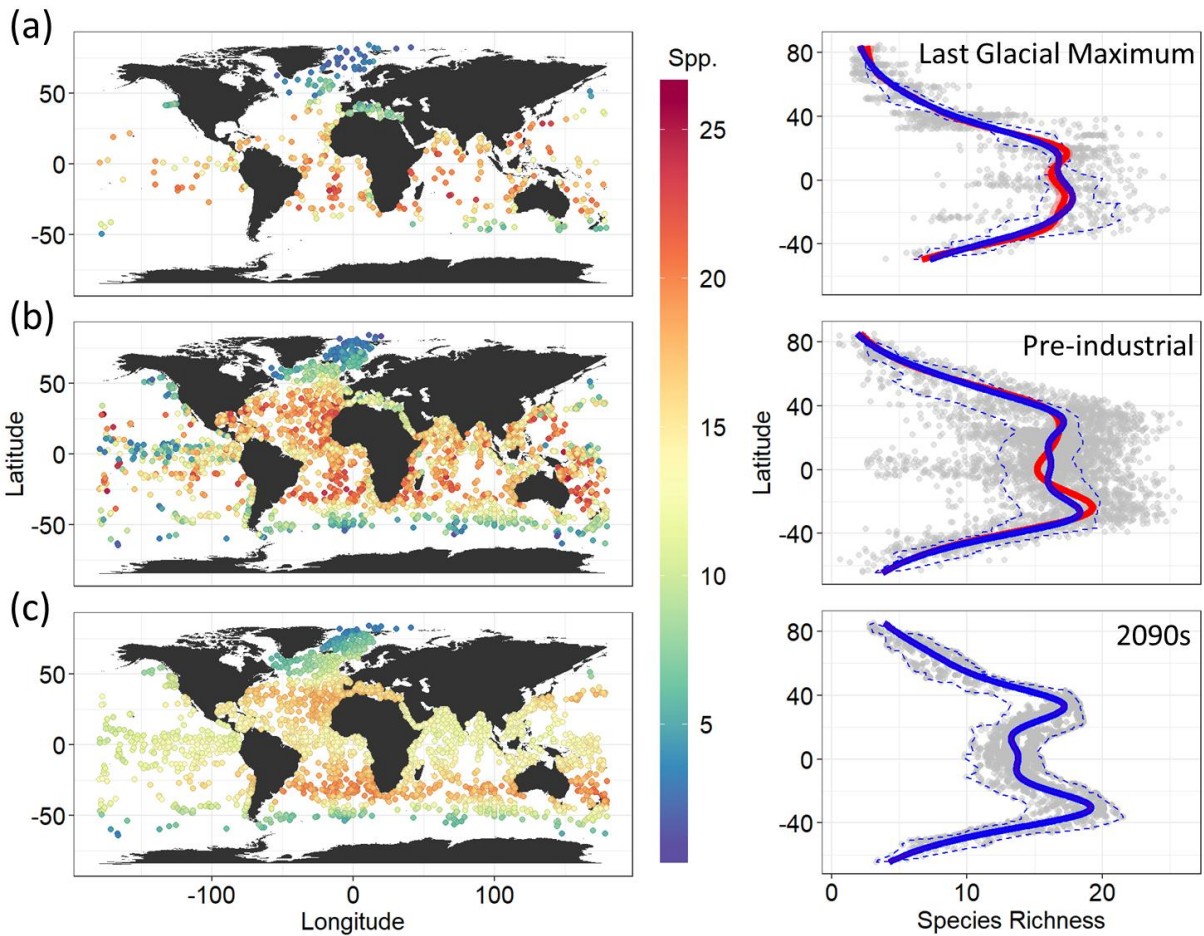
485
486 We decomposed beta-diversity (multiple-site Sorensen dissimilarity) which is influenced by
487 turnover and species richness, into spatial turnover (also called Simpson's dissimilarity index)
488 and nestedness components (57, 58). The beta-diversity measures and partitions were conducted
489 over a one-degree-latitude moving window. Within each moving window, five sites were
490 randomly resampled (with replacement) for 1000 times to estimate the mean and standard
491 deviation. Windows with less than five sites were omitted from the calculations. The same

492 analyses were tested across one- to five-degree-latitude moving window and show consistent
493 latitudinal patterns in beta diversity (SI Appendix, Fig. S4).

494
495 The latitudinal gradients of diversity were fitted by a generalized additive model (GAM) with a
496 quasipoisson error distribution, and a thin plate regression spline for the LGM and PIC datasets.
497 We also used a GAM to fit the LGM or PIC SST to their observed Hill numbers (e.g., species
498 richness or effective number of common species) to visualize the thermal gradient of diversity.
499 Finally, we constructed a third type of GAM using SST, longitude, latitude (and their interaction),
500 the ocean basins (i.e., Atlantic, Pacific, Indian, Arctic, and Southern Oceans) where the samples
501 were collected, and time (LGM and PIC) as predictor variables to account for spatial and
502 temporal diversity variations and to project the future distribution of species richness based on
503 the ensemble average of projected SST under RCP 8.5 and RCP 2.6 in the 2090s. The basis
504 dimensions in the GAMs was chosen ($k = 5$ or 6) to generate smooth curve fit for ease of
505 interpretation; nevertheless, the fitted lines are in general agree to the GAM with automatic
506 selection of k .

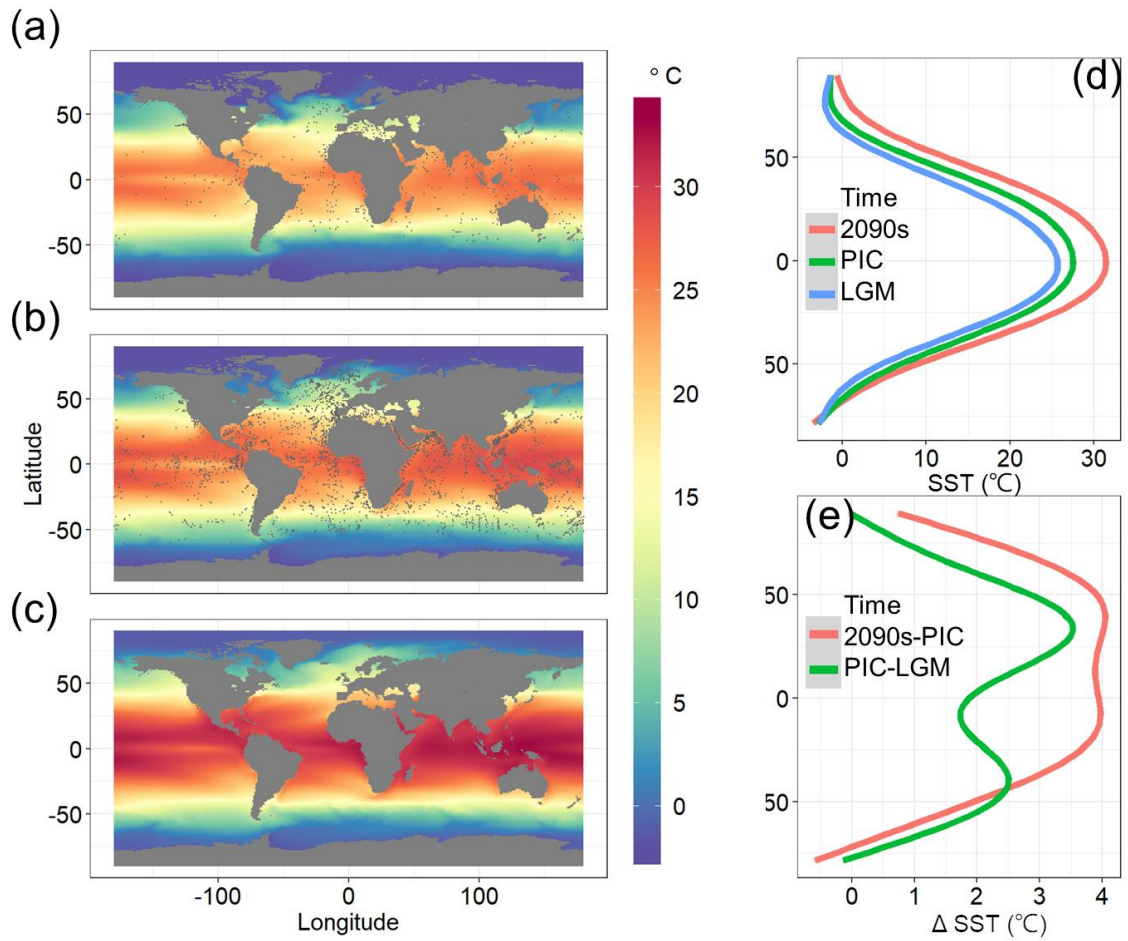
507
508 All statistical analyses were performed with R version 3.5.1 (59). Hill numbers and multivariate
509 analysis used the *vegan* package (60), beta-diversity the *betapart* packages (61), GAMs the *mgcv*
510 package (62), and GIS mapping and data visualization used the *raster*, *sp* and *ggplot2* packages
511 (63-65). A significance level of $\alpha = 0.05$ was applied to all statistical tests. All model residuals
512 were checked by standard diagnostic plots (i.e., residual vs. fitted values, qq plot) for
513 assumptions of homogeneity, independence and normal distribution, and by Moran's I test,
514 Moran's I spatial correlogram and variogram for spatial autocorrelation (66). The assumptions of
515 homogeneity, independence and normal distribution were reasonably met. Spatial
516 autocorrelations in the model residuals were detected at distances up to 2791 km for the LGM
517 and 1696 km for PIC species richness (Hill numbers of order $q = 0$) and up to 785 km for the
518 LGM and 1229 km for PIC effective number of common species (Hill numbers of order $q = 1$).

519
520 Dissolution of planktonic foraminiferal shells and upwelling may affect diversity. To
521 demonstrate that the diversity patterns were not affected by dissolution or upwelling, we ran the
522 same analysis for three subsets; namely samples with water depth less than 3000 m, those from
523 Atlantic Ocean only, and those excluding all coastal ecoregions, and thus coastal upwelling areas
524 (67). The shallow-depths and Atlantic subsets have higher calcium carbonate saturation state,
525 and thus better foraminiferal preservation (than the whole dataset including deeper depths and
526 other oceans than the Atlantic). The Atlantic Ocean does not have distinct low temperature zone
527 related to the equatorial upwelling, compared to the Pacific Ocean (Fig. 2). The results of these
528 subsets remain qualitatively the same (SI Appendix, Figs S5, S6, S7), showing that our results
529 are not artefacts of preservation or affected by upwelling.



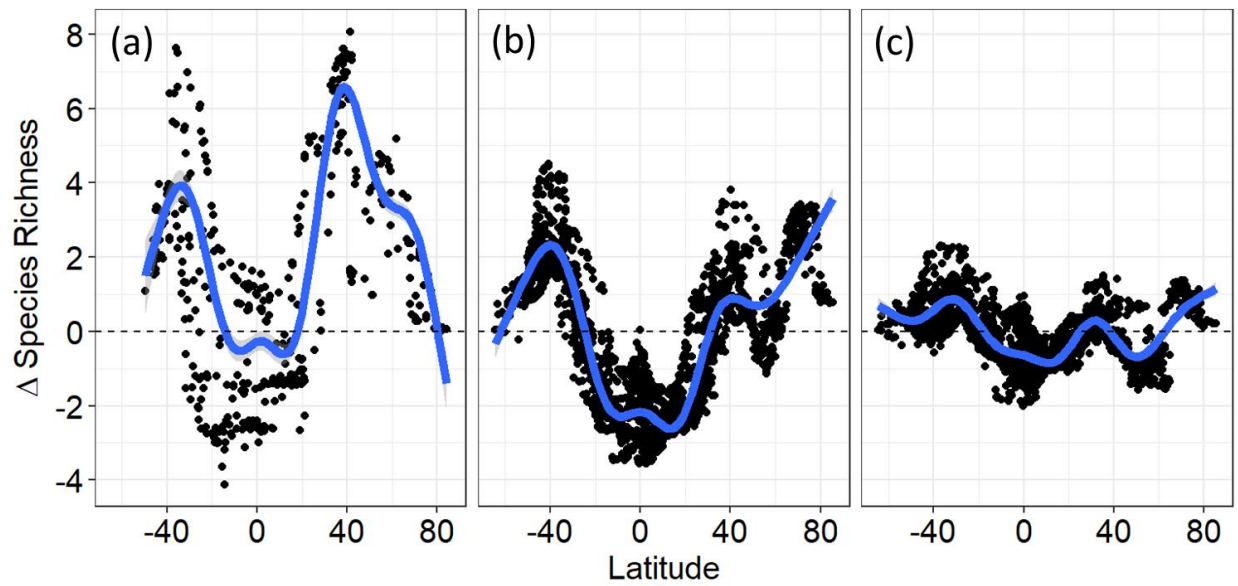
533
 534
 535
 536
 537
 538
 539
 540
 541
 542
 543
 544
 545
 546
 547
 548
 549

Fig. 1. Species richness of planktonic foraminifers during the (a) Last Glacial Maximum (LGM), (b) pre-industrial control (PIC), and for (c) 2091-2100 (2090s) as maps and latitudinal gradients. The observed diversities (LGM & PIC, gray symbols) were modeled by sea surface temperature, coordinates, and ocean basin using a Generalized Additive Model (GAM). The diversities in 2090s (gray symbols) were predicted from the same set of variables with future sea surface temperature (based on RCP 8.5). The predicted latitudinal diversities for the three time periods (enclosed by blue dashed lines) were smoothed by a GAM to show latitudinal diversity gradients (blue lines). The latitudinal gradient of observed diversities during the LGM and PIC were also fitted by a GAM and shown as the red lines with the shaded areas indicating the 95% confidence intervals (small and not visible in the PIC panel). LGM and PIC observations points have been had a small amount of jitter added on the x-axis to make them visible when overlapping. See SI Appendix Fig. S1 for empirical and projected diversities using a Hill number of order $q = 1$.



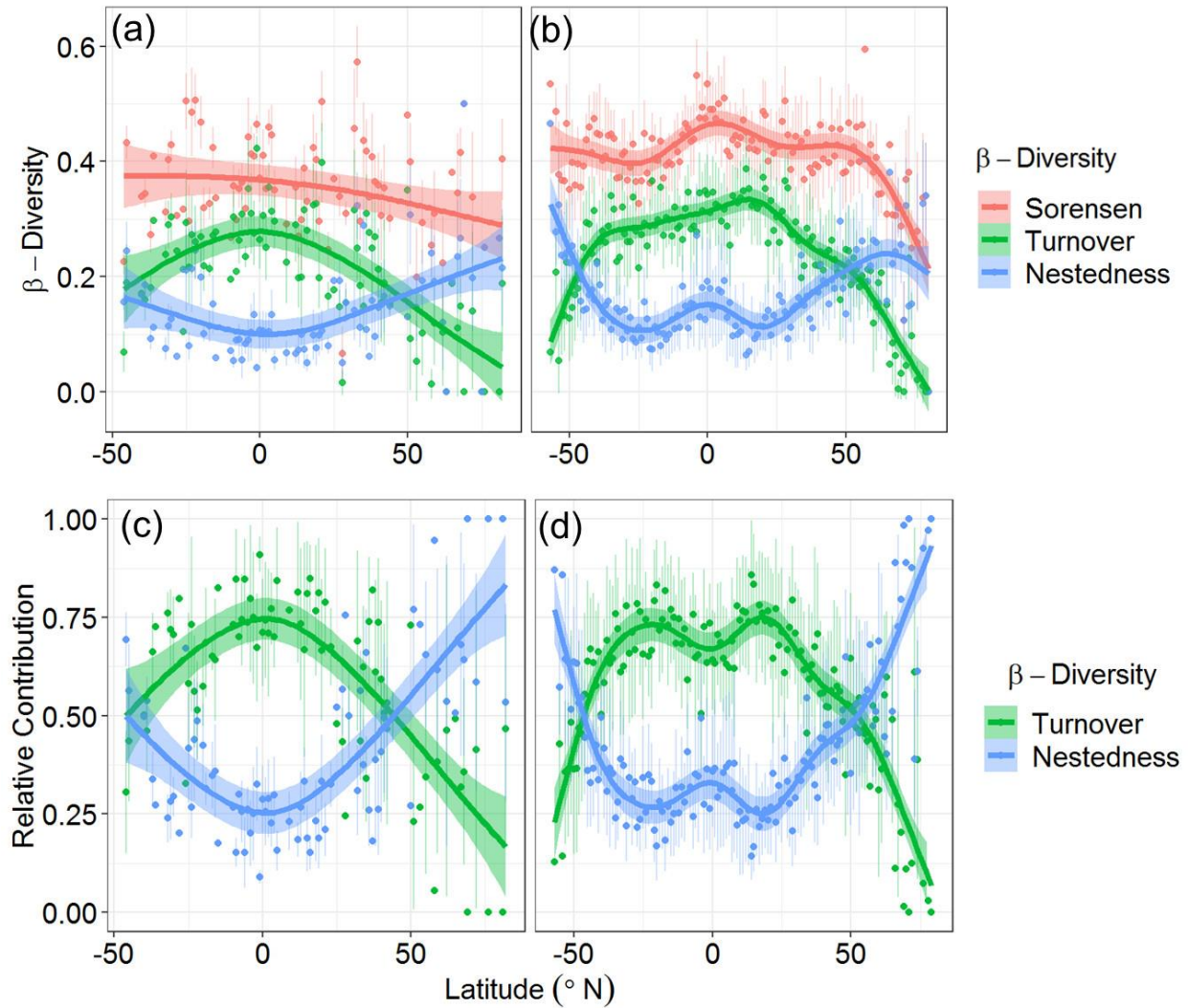
550
551
552
553
554
555
556

Figure 2. Maps and latitudinal gradients of the projected ocean sea surface temperature (SST) during the (a) LGM, (b) pre-industrial control (PIC), and (c) 2091-2100 (2090s) based on RCP 8.5. The latitudinal SST (LGM: blue; PIC: green; 2090s: red) and Δ SST (warming from the LGM to PIC as green and from the PIC to 2090s as red) are smoothed by a GAM and shown in panels (d) and (e), respectively. Grey dots in panels (a) and (b) indicate sample locations.



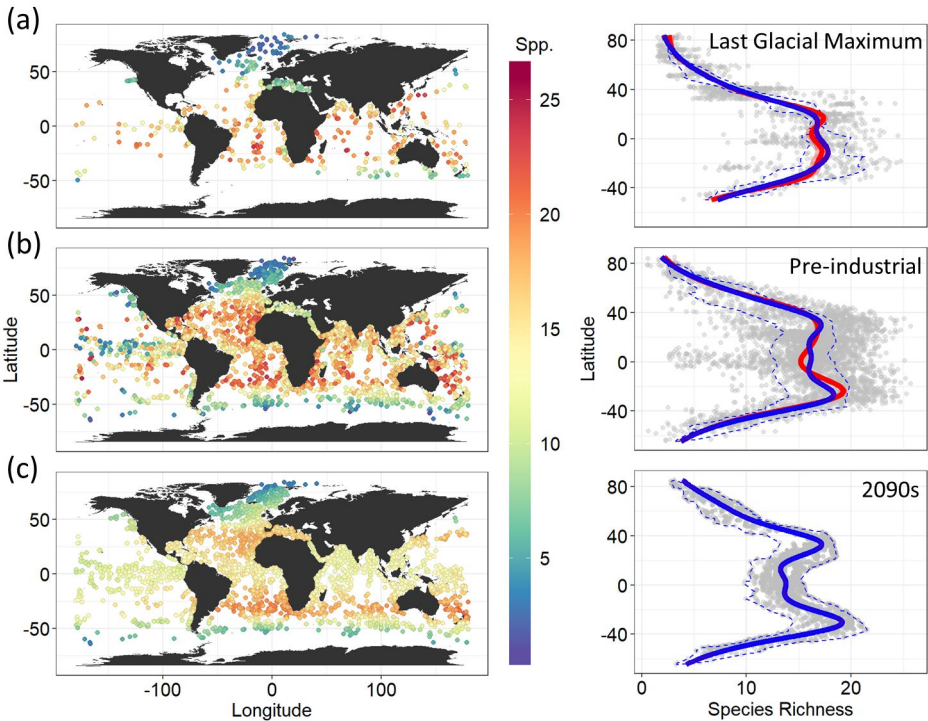
557
 558
 559
 560
 561
 562
 563
 564
 565
 566

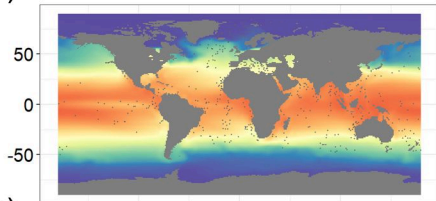
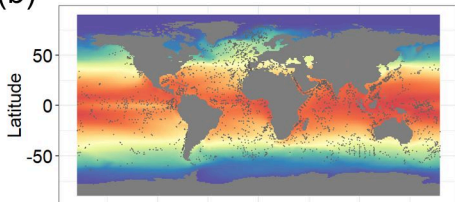
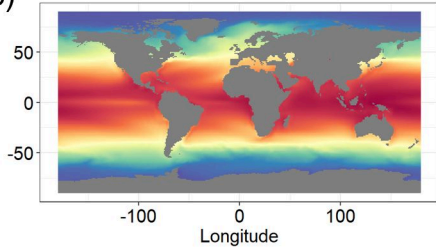
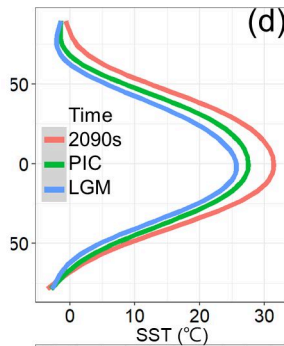
Figure 3. Changes in predicted species richness (Δ species richness) from the LGM to PIC (a), from the PIC to RCP 8.5 2090s (b), and from the PIC to RCP 2.6 2090s (c). Species richness was predicted using sea surface temperature for LGM, PIC, RCP 8.5 2090s, and RCP 2.6 2090s. The Δ species richness were calculated for the LGM samples in panel (a) and PIC samples in panel (b) and (c), and smoothed by a GAM [blue lines with the gray shaded areas indicating the 95% confidence intervals that are small and not visible in the panels (b) and (c)].



567
 568
 569
 570
 571
 572
 573
 574

Figure 4. The latitudinal gradients in beta diversity during (a) the LGM and (b) the pre-industrial periods. The total beta-diversity, i.e. Sorensen dissimilarity (red), was separated into turnover (green) and nestedness (blue) components. Panels (c) and (d) show the relative contribution of the turnover (green) and nestedness (blue) components to total dissimilarity for the LGM and pre-industrial periods, respectively.



(a)**(b)****(c)****(d)****(e)**